

Detectable close-in planets around white dwarfs through late unpacking

Dimitri Veras^{1*}, Boris T. Gänsicke¹

¹*Department of Physics, University of Warwick, Coventry CV4 7AL, UK*

Accepted 2014 November 21. Received 2014 November 18 in original form 2014 October 26

ABSTRACT

Although 25%-50% of white dwarfs (WDs) display evidence for remnant planetary systems, their orbital architectures and overall sizes remain unknown. Vibrant close-in ($\simeq 1R_{\odot}$) circumstellar activity is detected at WDs spanning many Gyrs in age, suggestive of planets further away. Here we demonstrate how systems with 4 and 10 closely-packed planets that remain stable and ordered on the main sequence can become unpacked when the star evolves into a WD and experience *pervasive inward planetary incursions throughout WD cooling*. Our full-lifetime simulations run for the age of the Universe and adopt main sequence stellar masses of $1.5M_{\odot}$, $2.0M_{\odot}$ and $2.5M_{\odot}$, which correspond to the mass range occupied by the progenitors of typical present-day WDs. These results provide (i) a natural way to generate an ever-changing dynamical architecture in post-main-sequence planetary systems, (ii) an avenue for planets to achieve temporary close-in orbits that are potentially detectable by transit photometry, and (iii) a dynamical explanation for how residual asteroids might pollute particularly old WDs.

Key words: minor planets, asteroids: general – stars: white dwarfs – methods:numerical – celestial mechanics – planet and satellites: dynamical evolution and stability – protoplanetary discs

1 INTRODUCTION

Our Solar system is packed. In other words, it could quickly become dynamically unstable with the insertion of an additional planet¹. Mounting discoveries of packed extrasolar systems (e.g. Lissauer et al. 2011, 2013; Swift et al. 2013; Cabrera et al. 2014; Masuda 2014) suggest that the Solar system is not unusual, particularly as detection sensitivities improve and formerly inaccessible discovery space is becoming available for exploration.

The concept of *packing* has received increasing attention over the last decade. Planet formation often appears to be efficient, even in the extreme environment of the first confirmed exoplanetary system (PSR B1257+12), discovered over two decades ago (Wolszczan & Frail 1992; Wolszczan 1994) around a supernovae remnant. The “packed planetary systems” hypothesis (Barnes & Raymond 2004; Barnes et al. 2008) advocates that efficient formation processes create planets with mutual separations that leave no room for additional companions. Dynamical scattering subsequent to formation represents another channel which can achieve tightly-

packed systems (e.g. Raymond et al. 2009a). The tally of packed systems continuously increases with observations that rely on transit photometry (Lissauer et al. 2011; Fang & Margot 2013), Doppler radial velocity measurements (e.g. Lovis et al. 2011; Anglada-Escudé et al. 2013) and even direct imaging (Marois et al. 2010). Now planetary packing has become the framework in which to analyse a variety of complex systems, such as those containing moons (Kane et al. 2013; Payne et al. 2013) or additional stars (Kratzer & Shannon 2014). Theoretical interest in the formation and evolution of these packed systems has also been robust (Hansen & Murray 2012, 2013; Chatterjee & Tan 2014; Hansen & Murray 2014; Hands et al. 2014).

The frequent occurrence of packed systems in nature motivates analyses of their ultimate fates. Although we do not yet have a confirmed detection of a planet orbiting a WD within a few thousand au² (Mullally et al. 2008; Hogan et al. 2009; Debes et al. 2011; Faedi et al. 2011; Steele et al. 2011; Fulton et al. 2014), we know that between 25%-50% of all white dwarfs (WDs), the end product of stellar evolution for over 90%

* E-mail: d.veras@warwick.ac.uk

¹ In fact, the long-term stability of the present Solar system is not guaranteed (Laskar & Gastineau 2009; Davies et al. 2013).

² Theoretical models constrain the mass of object WD 0806-661 b, which orbits a WD at a distance of approximately 2500 au, to the planetary mass regime (Luhman et al. 2011).

of all Milky Way stars, contain remnant planetary systems. This remarkable statistic follows from observations of abundant photospheric metal pollution in WD atmospheres (Zuckerman et al. 2003, 2010; Koester et al. 2014). These metals must be accreted from circumstellar matter, which is detected in a number of cases in the form of dusty (Zuckerman & Becklin 1987; Becklin et al. 2005; Kilic et al. 2005; Reach et al. 2005; Farihi et al. 2009) and gaseous discs (Gänsicke et al. 2006, 2007; Gänsicke 2011; Farihi et al. 2012; Melis et al. 2012). High levels of variability in these discs (e.g. Gänsicke et al. 2008; Wilson et al. 2014; Xu & Jura 2014) on timescales of years highlight the current dynamical activity occurring in these systems.

The debris discs, with a typical radial extent of about 1 Solar radius, cannot have existed during the main sequence or giant branch phases of stellar evolution. These discs are currently thought to originate from asteroids that are perturbed by planets onto highly-eccentric orbits (Bonsor et al. 2011; Debes et al. 2012; Frewen & Hansen 2014), whereupon the asteroids disrupt close to the WD (Graham et al. 1990; Jura 2003; Debes et al. 2012; Bear & Soker 2013; Veras et al. 2014a). The disc then accretes onto the WD (Bochkarev & Rafikov 2011; Rafikov 2011a,b; Metzger et al. 2012; Rafikov & Garmilla 2012; Wyatt et al. 2014), creating signatures of metal pollution. Pollution in WD systems without observed orbiting discs still somehow must arise from rocky planetesimals (Bergfors et al. 2014).

The presence of planets orbiting WDs on tight orbits would help explain asteroid delivery, but also raise the possibility of harbouring life by residing in a WD habitable zone (Monteiro 2010; Agol 2011; Barnes & Heller 2013). Fossati et al. (2012) has demonstrated that photosynthetic processes associated with complex life can be sustained on these planets. Further, because habitable WD planets would reside within 0.1 au, these planets are in principle more easily detectable by transit (Agol 2011) and by polarized or reflected light (Fossati et al. 2012). Biomarkers in the atmospheres of habitable planets transiting WDs might be observable with the James Web Space Telescope (Loeb & Maoz 2013). Indeed, JWST is capable of detecting objects with masses three orders of magnitude less massive than the Moon (Lin & Loeb 2014). However, so far, transit searches have been unsuccessful (Faedi et al. 2011; Fulton et al. 2014), and one theoretical prediction based on a simulation suite of three Jovian-mass planets suggests that less than 1 per cent of WDs host close-in Jupiters (see Section 4.3 of Mustill et al. 2014).

Motivated by both the robust signatures of remnant planetary systems and the possibility of detecting close-in planets, we here explore the link with packed planetary systems on the main sequence. First, however, we will review how long-term instability manifests itself in multi-planet systems, and comment on tidal effects between close-in planets and WDs.

1.1 Multi-planet instabilities

Before considering how multiple planets become unstable in post-main-sequence systems, we should understand instability on the main sequence (Davies et al. 2013). During a star’s main sequence lifetime, the star’s mass and radius change negligibly. These changes translate into little dynamical excitation amongst orbiting bodies; Veras & Wyatt (2012) point out that the So-

lar system planets would increase their semimajor axes by at most about 0.055 per cent. Due to such small changes, the vast majority of all main sequence exoplanet studies treat the stellar mass and radius as fixed. However, after the star leaves the main sequence, then the mass loss becomes extreme – causing orbital expansions by tens to several hundred percent, or outright ejection (Veras et al. 2011; Adams et al. 2013) – and the stellar radius increases by several orders of magnitude. Consequently, destabilization of planetary systems becomes more likely. In the Solar system, Mercury and Venus will be swallowed by the Sun, and Earth might too be destroyed (Schröder & Connon Smith 2008).

Here, we do not account for the gravitational effect of any residual smaller masses, such as planetesimals, asteroids or comets, on the planets: we treat our initial systems as already dynamically settled from formation. In reality, complex interactions between planetesimals and planets likely play important dynamical roles, primarily at the earliest main sequence ages; their incorporation enormously increases the available parameter space and computational cost of simulations (Tsiganis et al. 2005; Raymond et al. 2009b, 2010; Levison et al. 2011).

Stability boundaries are well-defined for two-planet systems. If the distance between two planets exceeds the Hill stability boundary, than those planetary orbits will remain ordered (non-crossing) forever (for a review, see Georgakarakos 2008), but not necessarily stable: the inner planet could collide with the star or the outer planet could escape. If that distance instead exceeds the Lagrange stability boundary, then the planets will forever remain bounded and ordered. The Hill stability boundary can be expressed in Jacobi coordinates for arbitrary eccentricities and inclinations (Donnison 2011) and is entirely analytical, except for a usually-negligible truncation in the expression of the energy (Fig. 19 of Veras et al. 2013a)³. Unfortunately, no such analytical formulation exists for Lagrange stability. However, empirical estimates (Barnes & Greenberg 2006; Veras & Mustill 2013) help establish this boundary. Also, two planets which are not Hill stable may still be bounded and ordered over long timescales. This behaviour is especially connected to the overlap of mean motion resonances (Chirikov 1979; Wisdom 1980; Mardling 2008; Funk et al. 2010; Mustill & Wyatt 2012; Deck et al. 2013; Giuppone et al. 2013; Bodman & Quillen 2014).

For systems with more than two planets, stability estimates become decidedly more imprecise. No analytical criterion exists like for the two-planet Hill stability case. Consequently, several authors (Chambers et al. 1996; Faber & Quillen 2007; Zhou et al. 2007; Chatterjee et al. 2008; Smith & Lissauer 2009; Quillen 2011) have attempted to fit empirical instability timescales to systems of three or more planets from numerical simulations. Because these estimates are primarily based on simulations with equal-mass planets, here we also adopt equal-mass planets in order to utilize these estimates. The rich dynamics in systems with a (more realistic) set of unequal-mass planets attests to its greater number of degrees of freedom (Veras & Armitage 2005, 2006;

³ Perhaps related is Marzari (2014)’s frequency map analysis finding that the dependence of the Hill boundary on planet mass has not yet fully been accounted for.

Ford & Rasio 2008; Jurić & Tremaine 2008; Raymond et al. 2011, 2012; Matsumura et al. 2013).

The dynamical complexities increase in post-main sequence systems, for which relatively few multi-planet studies have been performed. All such studies consider gravitational scattering which results from instability due to mass loss. Duncan & Lissauer (1998) investigated the future evolution of collections of planets in artificial Solar systems for various planet-Sun mass scalings. Debes & Sigurdsson (2002) evolved systems with two and three equal-mass planets over 1000 orbits around a progenitor $1M_{\odot}$ star that lost half of its mass in a uniform fashion. Veras et al. (2013a) evolved two-planet systems with equal planetary masses from the endpoint of formation to several Gyr into the WD phase for progenitor stellar masses of $3 - 8M_{\odot}$; this work was recently extended with simulations of equal-mass planets in three-planet systems (Mustill et al. 2014). Voyatzis et al. (2013) instead considered a more analytical approach, tracking the regular and chaotic trajectories in phase space that results from the inclusion of mass loss in multi-planet systems.

1.2 Tidal effects

Planets scattered close to their parent stars might change their orbits due to star-planet tides. Main sequence and giant branch studies dominate investigations of star-planet tidal dynamics; few references to WD-planet interactions exist. Nordhaus & Spiegel (2013) pose in their Section 4 that an Earth-mass planet driven to within half of a Solar radius (about 0.002 au) of an WD *might* be circularized due to tidal friction, but do not elaborate further on this process. They do surmise that the resulting dissipation of heat would render the planet uninhabitable, even if detectable. Mustill et al. (2014) suggest that the dynamics of WD-planet tidal interactions would be nearly equivalent to that of main sequence stars, and hence feature circularization, because the dominant forces arise from tidal deformation of the planet and not the star.

If we make that assumption here, then all of the uncertainties which plague tidal theory on the main sequence carry over to WD systems. This problem is compounded by the newfound inoperability or extremely limited scope (Efroimsky & Makarov 2013) of classic tidal theories such as the constant geometric lag model (Goldreich 1966; Murray & Dermott 1999) and the constant time lag model (Mignard 1979; Hut 1981). Consequently, a process such as tidal circularization of a terrestrial planet orbiting a WD must be taken on a case-by-case basis, one that is highly dependent on the rheology of the planet (but independent of the WD). The circularization timescale can easily vary by orders of magnitude depending on this rheology (Henning & Hurford 2014). Giant planets also suffer from this uncertainty, as they may contain solid cores, necessitating the combined modeling of fluid mechanics and solid mechanics. As observed by Ogilvie (2014), Earth's tidal dissipation is dominated by a fluid layer that represents just 0.023 per cent of the entire planet's mass.

Because our planets here represent point masses, we make no attempt to invent interior structures, nor compute maximum tidal reaches nor circularization timescales. Nevertheless, we emphasize throughout the manuscript that we neglect these processes, which may strongly affect planets that achieve pericen-

tres at orbital separations from the WD that are realistically within the reach of observational detection.

We now proceed to setup, execute and analyse our simulations in Section 2, discuss the results in Section 3 and conclude in Section 4.

2 SIMULATIONS

Our simulations incorporated self-consistently the evolution of both the host star and planetary orbits to model the progression of the planetary system throughout the main sequence, giant branch and WD phases. We performed integrations over the age of the Universe, which is approximately 14 Gyr.

2.1 Numerical code

We used an integrator with features from the simulators used in Veras et al. (2013a), Mustill et al. (2014) and Veras et al. (2014b). The integrator contains a Bulirsch-Stoer algorithm, originally from Chambers (1999), that is modified with stellar mass and radius interpolation between substeps. The stellar mass and radius profiles are computed with the *SSE* code (Hurley et al. 2000), assuming a Reimers mass loss prescription with coefficient 0.5 during early giant branch phases and a superwind prescription from Vassiliadis & Wood (1993) along the asymptotic giant branch phase. We assumed that the mass loss is isotropic, an excellent assumption for the planet-star separations considered in this paper (Veras et al. 2013b). When the star becomes a WD, the resulting (constant) radius is replaced with the WD's Roche radius assuming the planets all have a typical terrestrial planet density of 5.5 g/cm^3 (see Sect. 2.2.2). When a planet collides with the star, the star is modelled to absorb the planet and increase mass accordingly, affecting the subsequent dynamics of the system. Given the long duration of our simulations, we outputted data every 1 Myr, but importantly continuously tracked the minimum pericentre that every surviving planet ever achieved. We, conservatively, adopted a Bulirsch-Stoer tolerance parameter of 10^{-13} . Consequently, in every case, we have found that angular momentum was conserved to within 10^{-6} ; energy is not conserved in mass-losing systems.

2.2 Initial conditions

2.2.1 Stellar mass

Our choice of initial stellar masses in this work ($1.5, 2.0$ and $2.5M_{\odot}$) is an improvement over previous studies (Veras et al. 2013a; Mustill et al. 2014). The average mass of a WD in the present-day WD population is $0.60 - 0.65M_{\odot}$ (Liebert et al. 2005; Falcon et al. 2010; Tremblay et al. 2013), which corresponds to an A-type main-sequence progenitor star with a mass around $2M_{\odot}$ (Catalán et al. 2008; Kalirai et al. 2008; Casewell et al. 2009). Figure 1 of Koester et al. (2014) illustrates that by considering the stellar mass range of $1.5 - 2.5M_{\odot}$, we sample the progenitor mass range of nearly all known polluted WDs. This mass range corresponds to main sequence lifetimes between about 600 Myr and 3 Gyr. Consequently, the majority of the integration time was during the WD phase of

stellar evolution. The final WD masses corresponding to these initial main sequence masses are 0.576 , 0.637 and $0.690M_{\odot}$; the vast majority of the mass loss occurred on the asymptotic giant branch phase, as during the giant branch phase only 0.061 , 0.002 and $0.001M_{\odot}$ was shed.

2.2.2 Planetary mass and orbits

We adopted equal, Earth-mass planets ($3.0035 \times 10^{-6}M_{\odot}$) in our main suite of simulations; later we perform a few additional full-lifetime simulations with Jupiter-mass planets ($9.5460 \times 10^{-4}M_{\odot}$) in order to showcase the differences. We focus on terrestrial planets because (i) at the separations probed so far, low-mass planets appear to be much more common than giant planets (Winn & Fabrycky 2015), (ii) observational evidence for their packing is greater, and (iii) there already exist full-lifetime estimates for the critical survival separations throughout main sequence evolution for four or more terrestrial planets (Smith & Lissauer 2009).

Observationally, we are not yet sensitive to these planets⁴; terrestrial planets in regions beyond 1 au, such as Mars analogues, remain out-of-reach. Because super-Earths can form around Solar-type stars out to 5 au (de Elía et al. 2013), formation of Earth-like planets around more massive stars should take place *beyond* 5 au. In fact, the snow or ice line – a concept often used to demarcate the formation of terrestrial from giant planets – changes distance with time, but can reach a distance of up to 10 au after 10^5 yr for the stellar masses we considered (Kennedy & Kenyon 2008). For terrestrial planets which emerge from their birth disc, Kokubo & Ida (1998) show that separations of 10 mutual Hill radii are typical. In order to estimate our mutual Hill radii, we utilised the definition from equation (4) of Smith & Lissauer (2009), which reads

$$a_{i+1} = a_i \left[1 + \frac{\beta}{2} \left(\frac{m_i + m_{i+1}}{3(m_{\star} + \sum_{k=1}^{i-1} m_k)} \right)^{1/3} \right] \times \left[1 - \frac{\beta}{2} \left(\frac{m_i + m_{i+1}}{3(m_{\star} + \sum_{k=1}^{i-1} m_k)} \right)^{1/3} \right]^{-1} \quad (1)$$

where m and a refer to mass and initial semimajor axis, subscripts refer to planets in order of increasing distance, and β is the number of mutual Hill radii. Four Earths orbiting a Solar-mass star with $a_1 = 1$ au, $\beta = 4$ corresponds to $(a_2, a_3, a_4 = 1.05, 1.11, 1.16)$ au whereas $\beta = 10$ instead corresponds to $(a_2, a_3, a_4 = 1.13, 1.29, 1.46)$ au. If the planets were instead Jovian, then $\beta = 10$ would correspond to $(a_2, a_3, a_4 = 2.51, 6.29, 15.8)$ au.

The process of unpacking is largely scale-invariant, i.e. independent of our choice of a_1 . However, there do exist physical constraints. Johansen et al. (2012) and Petrovich et al. (2014) show an increased incidence of collisions with the central star as a_1 is decreased, a phenomenon which can be explained through the Safronov number (Safronov & Zvjagina 1969). This number

Table 1. Summary of simulations, four per row. Each simulation contains either Earth-mass planets or Jupiter-mass planets, separated by a mutual Hill separation indicated by β through equation (1). If β is too large, instability will never occur. If β is too small, the first instability will occur quickly (i.e., on the main sequence; MS).

Terrestrial planets					
Row #	# of planets	progenitor mass (M_{\odot})	β	a_1 (au)	% unpacked on post-MS
1	4	1.5	10	5	75
2	10	1.5	10	5	100
3	4	2.0	10	5	100
4	10	2.0	10	5	100
5	4	2.5	10	5	100
6	10	2.5	10	5	100
7	4	1.5	10	10	25
8	10	1.5	10	10	100
9	4	1.5	12	5	25
10	4	1.5	15	5	0
11	4	2.0	12	5	100
12	4	2.0	15	5	25
13	4	2.5	12	5	100
14	4	2.5	15	5	0
Giant planets					
15	4	1.5	8	5	0
16	4	2.0	8	5	0
17	4	2.5	8	5	0
18	4	1.5	6	5	100
19	4	2.0	6	5	100
20	4	2.5	6	5	100
21	4	1.5	4	5	0
22	4	2.0	4	5	0
23	4	2.5	4	5	0

represents the square of the ratio of orbital speed to surface escape speed. As this ratio increases, the frequency of collisions increases.

Another constraint includes star-planet tides along the post-main-sequence phases, as a star’s radius will expand significantly and might swallow the planet. For the stellar mass range we consider ($1.5 - 2.5M_{\odot}$), a terrestrial planet with a circular orbit and main sequence semimajor axis of at least about 3 au will survive engulfment from the expanding giant star (Figure 7 of Mustill & Villaver 2012). This bound remains robust even for different mass loss prescriptions (Adams & Bloch 2013; Villaver et al. 2014). Another constraint is the age of the Universe, which limits the total number of orbits which could be completed as a function of a_1 , affecting Lagrange-type instability (e.g. Veras & Mustill 2013). However, as the number of orbits increase, computations take longer and may accumulate error in angular momentum conservation.

For these reasons, we choose $a_1 = 5$ au for most of our simulations; $\beta = 10$ then gives $(a_2, a_3, a_4 = 5.67, 6.44, 7.30)$ au.

We do not include Galactic tides in our simulations, as planets in the Solar neighbourhood are negligibly perturbed by these tides for separations up to thousands of au (Kaib et al. 2013; Veras & Evans 2013a,b), and adiabatic mass loss will increase the outermost planet’s initial semimajor axis [$a_{10} < 20$

⁴ See the Exoplanet Data Explorer at <http://exoplanets.org>.

au] by a factor of just a few. The outcomes of our simulations justify this choice *ex post facto*. We also do not include flybys from passing stars, for both computational reasons and so that we can focus on the unpacking process. In reality, we should expect, over the age of the Universe, one Galactic field star to come within a few hundred au of another (Zakamska & Tremaine 2004; Veras & Moeckel 2012). However, post-main-sequence mass loss occurs for just a small fraction of this time. Therefore, during post-main-sequence mass loss, a stellar flyby would not be expected to penetrate to within 10^4 au in the Solar neighbourhood (Veras et al. 2014c).

Our simulations also do not include the effect of general relativity (GR). During the course of each orbit, GR can displace a highly eccentric planet from its predicted pericentre location around a typical $0.6M_{\odot}$ WD by up to 2.65 km (Veras 2014). This value is independent of the planet's semimajor axis or pericentre. Other changes to the orbit during one complete period are similarly minor. However, over many orbits, the pericentre may precess noticeably; the extent of this precession is in fact dependent on the semimajor axis and eccentricity. Equation 19 of Veras et al. (2014a) demonstrate that any highly-eccentric object approaching the Roche radius of the WD can experience precession on the order of a few degrees within 10^5 yr. Consequently, any secular behaviour which is strongly dependent on the argument of pericentre, such as the Lidov-Kozai mechanism, could be affected by GR.

Unlike Smith & Lissauer (2009), we initialized our planets on slightly non-coplanar orbits. We drew inclination values from random uniform distributions with ranges of $[-0.5^{\circ}, 0.5^{\circ}]$ in order to avoid an artificially high number of collisions, given that real systems are not exactly coplanar but tend to harbour planetary orbits which are mutually inclined on the order of degrees⁴. We performed a similar random selection for all orbital angles (mean anomaly, argument of pericentre, longitude of ascending node) over their entire ranges. We set the planets on initially circular orbits for simplicity and because Jurić & Tremaine (2008), among others, suggest that qualitative scattering outcomes are independent of initial eccentricity.

2.3 Simulation results

2.3.1 Terrestrial planet suite

Here we discuss the results of our main set of simulations, summarized in Table 1, and show two illustrative evolution examples in Fig. 1. Figure 2 summarizes the results from the majority of the simulations in the table. We performed four simulations with slightly different initial conditions (Sect. 2.2.2) for each set of parameters, i.e. for each row in Table 1. Within each row, the number of planets as well as the values of M_{\odot} , β and a_1 were fixed.

The table reveals that our choice of 10 mutual Hill radii successfully keeps the planets ordered and packed along the main sequence, before unpacking occurs along the post-main-sequence phases. Rows #9, #11 and #13 indicate that increasing β to 12 reproduces similar behaviour. When $\beta = 15$, the planets are too widely separated to ever unpack, except in a single case (see rows #10, #12 and #14). The finding that unpacking ceases when $12 < \beta < 15$ is in line with the prediction from Fig. 11 of Mustill et al. (2014) after their single-planet Hill radii is con-

verted into the mutual-planet Hill radii used here (originally from Smith & Lissauer 2009). Doubling the value of a_1 , as in rows #7-#8, still produces unpacking in all four 10-planet cases, but in just one of the 4-planet cases. The likely reason is because these planets have not completed as many orbits (see Fig. 6 of Veras et al. 2013a and Veras & Mustill 2013). Altering the stellar mass does not have a significant effect on the final unpacking statistics, but dramatically changes the main sequence lifetimes and therefore the possible extent of the WD cooling ages. Nevertheless, comparing the last column in the first 6 rows suggests that the amount of mass lost from $1.5M_{\odot}$ progenitor mass stars was just not high enough to produce unpacking in every case (Row #1)⁵.

Figure 1 provides two examples of the time evolution of individual simulations from rows #1 and #6. The plots visually demonstrate that the main-sequence lifetimes of the $1.5M_{\odot}$ and $2.5M_{\odot}$ stars are roughly 3 Gyr and 0.6 Gyr. Along this phase, the planets remain ordered and packed.

Now consider the upper panels in more detail. The 4 planets here remain in this effectively stable state throughout both the giant branch phases, when their semimajor axes are more than doubled, and through nearly 3 Gyr of WD cooling. Only after this time do the planets unpack, crossing one another's orbits. Subsequently, the planets' orbital eccentricities are excited, and some planets sweep inwards towards the WD at distances much less than the original innermost orbit ($a_1 = 5$ au), or even the maximum stellar radius ($R_{\max} = 1.42$ au). Eventually, the initially outermost planet enters the Roche radius of the WD ($R_{\text{roche}} = 0.0035$ au) at 12.2 Gyr, corresponding to a cooling age of about 9 Gyr.

Contrastingly, in the bottom panels, the initially packed system of 10 planets becomes unpacked during the giant branch phases, and specifically during the asymptotic giant branch phase⁶. With 10 planets and a high maximum amount of total mass lost, the stability boundary is more easily critically shifted than in the 4-planet case with a smaller maximum amount of mass lost. During the entire WD phase, lasting over 13 Gyr, the inner system is swept through by planets on eccentric orbits. Three of these planets hit the Roche radius of the WD, at 5.61 Gyr, 6.19 Gyr and 9.72 Gyr, at which point the planets are absorbed into the WD and increase its mass. One of the planets (red) which survives for the age of the Universe drifts within 0.05 au of the WD at 10.68 Gyr. A planet with such a close pericentre has a non-negligible probability of being detected while transiting the WD. If the pericentre is close enough to the WD for tidal circularization to occur, then prospects for detection increase dramatically. As the orbit circularizes, the geometric transit probability remains the same, while the transit duration increases and the orbital period decreases (Barnes 2007; Socrates et al. 2012); the latter effects provide the enhancement in detectability.

All instabilities manifested themselves as planet-planet collisions or planet-star collisions; no planets were ejected. Ejections require planets to be scattered out to large distances from

⁵ More precisely, in one case the mass loss failed to shift the stability boundary sufficiently enough to cause orbit crossing either during a giant branch or WD phase.

⁶ None of our simulations were destabilized along the Red Giant Branch phases.

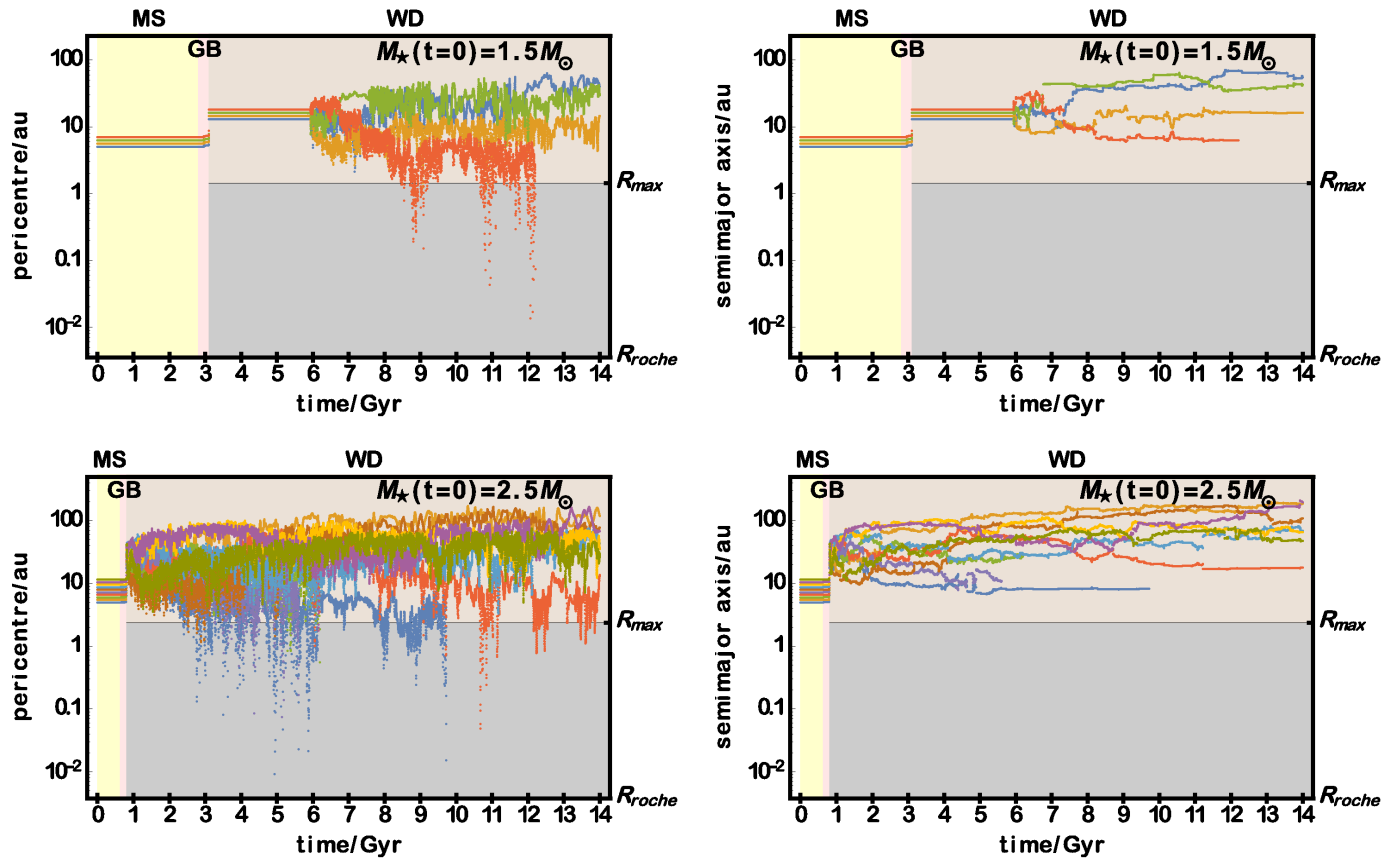


Figure 1. Two examples of post-main-sequence planetary unpacking with terrestrial planets. The top and bottom panels each correspond to one simulation from rows #1 and #6 of Table 1, respectively. The background colours refer to the main sequence (MS; yellow), giant branch (GB; pink) and white dwarf (WD; gray) phases of stellar evolution. In the top panels, the 4 planets remain packed for the entire MS and GB phases, and for about 3 Gyr of WD evolution. In the bottom panels, the 10 planets become unpacked during the GB phases (specifically, during the Asymptotic Giant Branch). In both cases, planets make sweeping incursions well within the initial innermost semimajor axis and maximum stellar radius R_{\max} , and at WD cooling ages exceeding 5 Gyr. In the top left panel, the initially outermost planet (red) spent Gyrs of WD cooling time at close pericentres before being engulfed into the WD at 12.2 Gyr. The bottom-left panel features a particularly intrusive incursion: the dark blue planet achieves a pericentre of 0.046 au – close to a typical WD habitable zone and beyond the WD Roche radius R_{roche} – at 10.68 Gyr, and survives. Depending on the internal properties of the planet, it might be subsequently tidally circularized - a process ignored in this work. The semimajor axis evolution showcase the complex energy exchanges triggered in these systems after the first instance of instability, and demonstrate that close pericentre passages are due to variations in orbital eccentricity.

the star, and these distances were not attained with the terrestrial planets simulated here. Our integrator faithfully tested for ejections by incorporating the true Hill escape ellipsoid in the Solar neighbourhood, with semi-axes on the order of 10^5 au (Veras & Evans 2013b). Therefore, planets flung out on orbits of several hundred au are retained (see, e.g. the bottom right panel of Fig. 1). Further, Ford & Rasio (2008) suggest that the smaller the planets, the less likely ejection is to occur. Finally, stellar mass loss by itself is not fast and great enough to cause escape due to both the physical properties of the stars simulated and the planetary orbits considered (Veras et al. 2011). Of the instabilities across all terrestrial planet simulations, three quarters were engulfments into the star, and one quarter were planet-planet collisions. Planet-planet collisions are a plausible avenue to generate large amounts of fresh small body debris,

which could explain strong metal pollution detected in a number of old, cool WDs (Koester et al. 2011).

We can improve our understanding of the dynamical evolution in both panels by focusing on the planetary semimajor axis changes throughout the star’s lifetime (right panels of Fig. 1). Although a system’s total orbital energy includes eccentricity-dependent and inclination-dependent planet-planet interaction terms (see e.g. equation 2.27 of Veras 2007), we can use the other terms, whose only orbital parameters are semimajor axes, as excellent proxies (see Fig. 19 of Veras et al. 2013a) for energy transfers in the system. Further, after the star has become a WD, and mass loss ceases, energy is conserved for the remainder of the system’s existence. In Fig. 1 the semimajor axes “jump” around in a vaguely sawtooth-like manner, indicating shifts in orbital energy due to instances of strong interactions with the other planets.

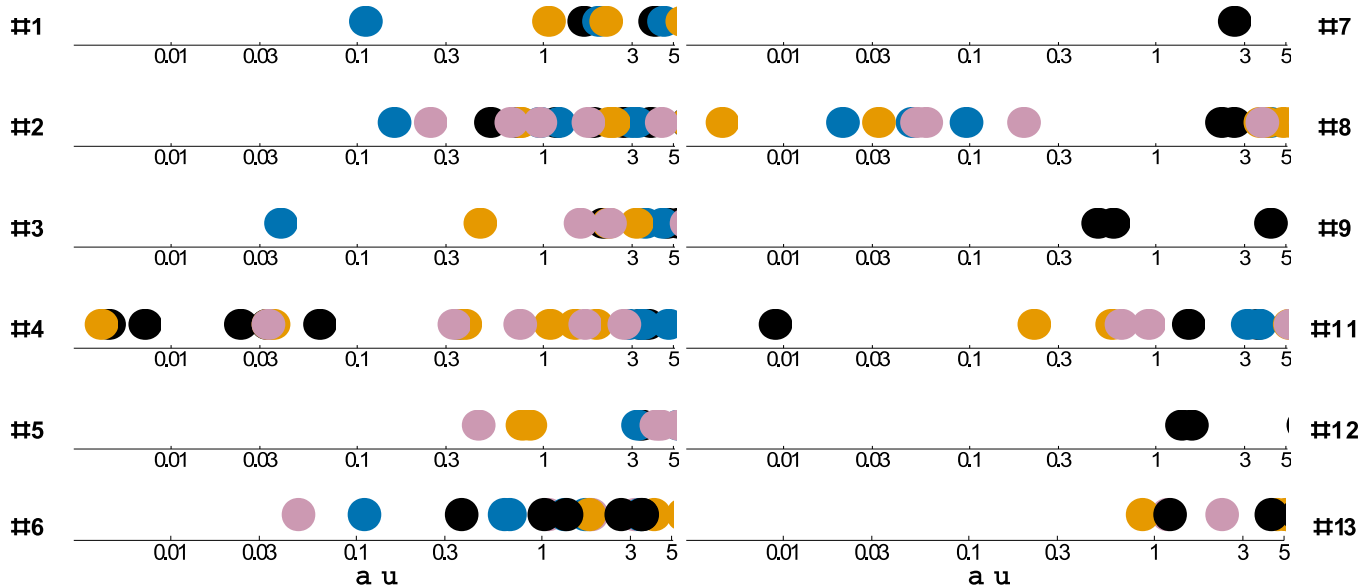


Figure 2. Minimum pericentres (in au) which are less than 5 au for systems in Table 1. Each numberline corresponds to a different (labelled) row of the table (rows #10 and #14 did not unpack), and each numberline displays all planets in all four runs of a given row; each run is colour-coded. Note that even for rows #7 and #8, where $a_1 = 10$ au, at least one planet achieves a minimum pericentre within 5 au. This figure demonstrates that an endemic feature of post-main-sequence unpacking is inward incursions of one or more planets to values which are just a fraction of their original main sequence semimajor axes.

In the upper right panel, after an initial period of orbit crossing lasting a few Gyr, the planets’ orbits remain largely ordered, except for one notable orbit crossing at just over 11 Gyr. In no instance is the semimajor axis of a planet perturbed down to values within a few au. This result is expected because when the planets’ orbits are ordered and not undergoing strong interactions, they are evolving secularly, and secular interactions do not alter semimajor axes. Also, during scattering the apocentre must remain high in order to interact with the other planets. Hence, the semimajor axis cannot be reduced by much more than 50 per cent. Therefore, the small pericentres achieved are due primarily to changes in orbital eccentricity and not semimajor axis. Nevertheless, this analysis neglects the effects from tidal circularization, which may effectively “grab” a planet at its pericentre and keep that pericentre to within a factor of 2 while shrinking the orbital semimajor axis.

Regardless of semimajor axis, the minimum planetary pericentre is the value of greatest interest here because of (i) how close-orbit planets might potentially perturb asteroids into the Roche radius of the WD, and (ii) the possibility of detecting these planets (Agol 2011; Fossati et al. 2012). Therefore, we present a collection of these minimum pericentres in Fig. 2 for all simulations that became unpacked and for all planets that have survived for the age of the Universe. For each of 7 different numberlines (sets of initial conditions), at least one simulation featured an incursion within 0.1 au of the star. In one 10-planet simulation (row #2), 5 of the surviving planets each individually drifted to within 5 au of the star. Each numberline demonstrates a wide variation of behaviour across the simulations, perhaps emphasising the highly chaotic nature of unpacked planetary systems.

2.3.2 Selected giant planet simulations

We performed some additional simulations, this time with packed giant planets, in order to determine how the process of unpacking changes for a higher planet/star mass ratio. In these simulations, we assumed a WD Roche radius based on a typical giant planet density of 1.0 g/cm^3 . There are two particularly strong cases of packed giant planets which act as observational motivation: our solar system, and the HR 8799 system (Marois et al. 2008, 2010).

We found that closely-packed giant planets which remain stable throughout the main sequence before undergoing instability require $\beta < 8$. These lower values differ from the terrestrial case probably because the Hill sphere is no longer the relevant parameter governing the dynamics; see equation 2 of Faber & Quillen (2007) for the explicit dependence on planet mass. The predictions for stability of post-MS systems based on this equation seem to agree with the results presented in the present paper for giant planets too (see Fig 11 of Mustill et al. 2014). We also find that giant planet unpacking is more violent than terrestrial planet unpacking, resulting in less orbit meandering, speedy dynamical settling following instability, and escaping planets⁷.

Figure 3 illustrates two specific examples. For both cases,

⁷ The stronger close encounters likely decrease the accuracy of the simulations; here, typically total angular momentum is conserved to only $10^{-4} - 10^{-3}$. These values indicate that future studies modeling full-lifetime simulations containing strong interactions amongst many giant planets would benefit from either tiny Bulirsch-Stoer tolerances ($< 10^{-13}$) – prolonging the simulations even further – or by utilizing other codes. One may combine planetary and stellar evolution codes in the AMUSE package (Pelupessy et al. 2013), or modify an exist-

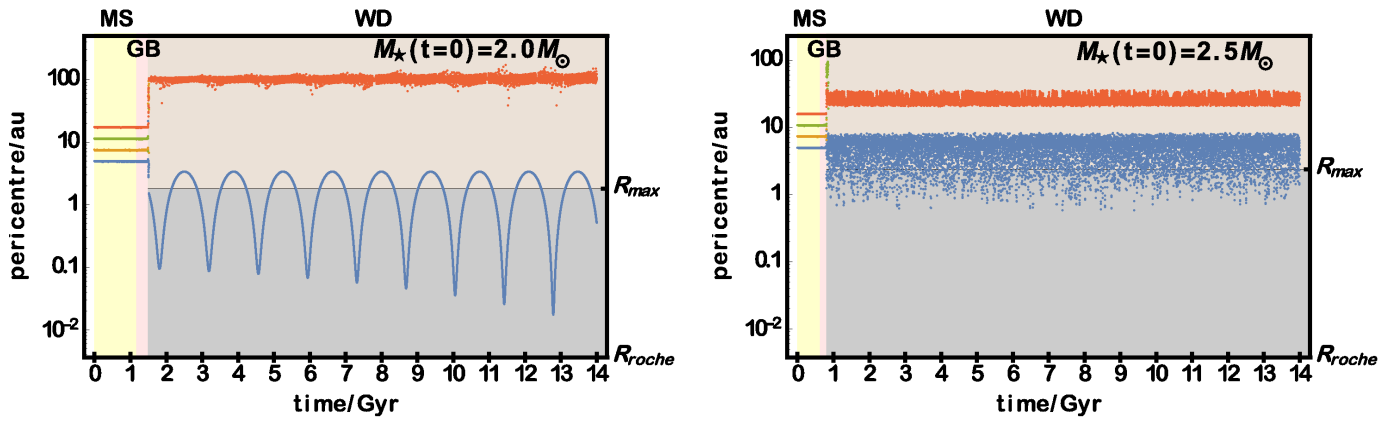


Figure 3. Two examples of post-main-sequence planetary unpacking with Jovian planets, from Rows #19-#20 of Table 1. Both panels feature four planets with initial semimajor axes between 5 au and 17.38 au (left panel) or 5 au and 15.86 au (right panel). In both cases, instability occurs only after the star has become a WD and already shrunk its radius down from its maximum value R_{\max} to approximately that of the Earth. In the left panel, the inward incursions of the initially innermost planet are periodic with increasing penetration. Alternatively, in the right panel, the incursions are more frequent and irregular. Neither GR nor tidal forcing is included in these simulations, which may affect the evolution of the simulation in particular in the left panel.

$\beta = 6$, and the instabilities in the system occur during the WD phase, *after* the stellar radius has been reduced to approximately Earth-size. In both cases, two planets are ejected, and one remaining planet is perturbed onto a wide orbit. The other planet experiences eccentric excursions close to the WD, and may be tidally circularized depending on the internal properties of the planet and its orbital pericentre.

The manner in which the incursions take place can be periodic and well-defined (left panel) or irregular and frequent (right panel). The oscillations in the left panel have an increasing amplitude, suggesting a way for giant planets to potentially collide with a WD after 10 Gyr of evolution. An event of this kind would give rise to a noticeable optical (and probably X-ray) transient, and result in a dramatic amount of metal pollution of the WD photosphere. Such large and periodic eccentricity variations are classic signatures of Lidov-Kozai oscillations (see Section 7 of Davies et al. 2013 for a review); figure 4 confirms this suspicion with accompanying inclination oscillations. The changing amplitude may be indicative of the role of the octupole term in Lidov-Kozai evolution (see Fig. 10 of Naoz et al. 2013). Of note is that when the orbit pericentre is at a minimum, its inclination is also at a minimum. Then we might expect a detectable planet in this case to harbour an inclination at the critical Lidov-Kozai value, around 40 degrees. Because this mechanism is strongly dependent on the evolution of the argument of pericentre, the evolution of this particular system may have been different had we included GR in our simulations.

If tidal circularization is an active process in WD systems, then the inclinations of highly eccentric planets will be preserved as they are circularized. The reason is that inclination damping is primarily due to tides raised on the star, which are weak for WDs (as they are for main sequence stars). Consequently,

ing planetary integrator that emphasizes greater speed and accuracy (Grimm & Stadel 2014; Rein & Spiegel 2014).

close-in planets orbiting WDs might harbour a broad range of inclinations.

3 DISCUSSION

Our results demonstrate that planets can be perturbed onto orbits taking them close to the WD at late ages, after an entirely quiescent existence. This finding is particularly important in the context of observations of *old* WDs with extreme metal pollution (Koester et al. 2011 and Fig. 8 of Koester et al. 2014) or orbiting debris discs (e.g. Farihi et al. 2011). If asteroids are the progenitors of the pollution and the discs, then the asteroids must be flung towards the WD, and probably by a planet.

One effective way to deliver asteroids is with a planetary mean motion resonance (Debes et al. 2012). Inside of a resonance, asteroid eccentricities can be pumped high enough to eventually achieve a WD-skimming orbit. This physical process, when applied to a single planet and an asteroid or Kuiper belt, produces a gradually decreasing stream of asteroids due to a depleting reservoir. Only a massive-enough belt would be able to sustain a high-enough delivery rate to explain accretion in WDs which are many Gyr old.

An alternative to resonant diffusion is direct scattering. However, a single planet will never change its orbit, except during giant branch mass loss, due to interactions with a relatively massive planetesimal belt, or due to a flyby star. Therefore, scattering between a single planet and an asteroid belt will occur at young WD cooling ages (Bonsor et al. 2011; Frewen & Hansen 2014). Penetrative stellar flybys can scatter the planet, thereby refreshing planet-asteroid dynamics in the system, but only for favourable geometries, and infrequently (Veras & Moeckel 2012).

Neither single-planet scattering, nor resonant diffusion commencing when the WD is born, can easily explain pollution or discs which exist around WDs that are many Gyr old. Multi-

planet systems, in concert with smaller bodies, may represent a solution. Two-planet systems are likely to be inadequate, because after an instance of instability, the surviving planet will have a fixed orbit, akin to the one-planet case. Although this orbit can be highly eccentric and penetrate to within the maximum radius of the star (Veras et al. 2013a), the orbit is periodic, and will too-quickly exhaust its supply of fortuitously-located asteroids. Three-planet systems are more promising because after instability, two surviving planets can exist in ever-changing orbits for the entire WD cooling age (Mustill et al. 2014), similar to the behaviour here in the right panel of Figure 3. Nevertheless, if these two surviving planets are secularly evolving, they will experience predictably periodic changes in their orbits (left panel of Figure 3).

Systems with at least four planets appear to harbour dynamics which are rich enough to potentially generate dynamical interactions with asteroids over long timespans and over an extensive range of physical space. Given the four terrestrial planets in the Solar system, and the mounting discoveries of packed exosystems, such configurations are perhaps common. Indeed, over half of all stars in the Milky Way are thought to contain at least one terrestrial planet (Cassan et al. 2012), and perhaps an average of at least five (Ballard & Johnson 2014). This average may be even higher considering that Ballard & Johnson (2014) focussed on M dwarfs, which have much lower masses than the stars considered here. Further, the asteroidal material in the remnant WD system may be widely dispersed and have a size distribution skewed towards small bodies due to rotational fission from giant branch radiation (Veras et al. 2014d). Consequently, rocky material may be available in enough locations to be accessed at different times during WD cooling.

Our simulations also provide a potential evolutionary pathway – a dynamical history – for eccentric planets which could be tidally circularized, then they would not remain in a secularly stable compact configuration for Gyrs. Instead, their pericentres would drift by orders of magnitude, greatly reducing their prospects for habitability. Consequently, observations would have to “catch” a system at just the right point in its secular evolution (e.g. Veras & Ford 2009). We suggest that detectable eccentric planets would likely be accompanied by an unseen outer companion. The prospects for detection will increase with current and upcoming missions such as Gaia, LSST and PLATO, which will survey $10^5 - 10^6$ WDs tens to thousands of times.

4 CONCLUSIONS

We find that the post-main-sequence peregrinations of terrestrial planets which were packed and quiescent throughout the main sequence cover a large volume of space at both early and late WD cooling ages. These planets often but irregularly invade regions which are well-interior to their nascent orbits and potentially contain asteroidal material that remained largely unperturbed for the entire main sequence and giant branch phases of stellar evolution. Consequently, these disturbances could represent catalysts for dynamical interactions which lead to the formation of debris discs and/or atmospheric pollution in old WDs. The planets themselves, when traveling through the pericentres of their orbits during epochs of high eccentricity, should

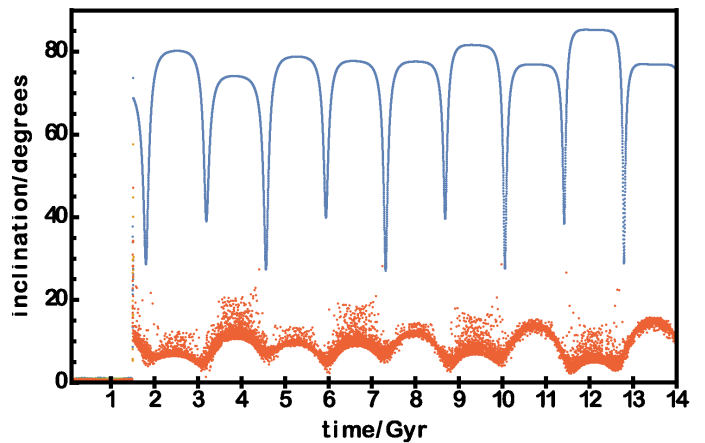


Figure 4. Lidov-Kozai oscillations of inclination from the left panel of Figure 3. The interplay between the inclination and eccentricity variations result in close pericentre passages around the WD in this one case when two planets survive instability.

be detectable and might be tidally circularized, but are unlikely to harbour life.

ACKNOWLEDGMENTS

We thank the referee for a thorough and thoughtful review, explicit and constructive comments, and an expeditious response to our submission. We also thank Alex Bowler for pointing out a typographic error in Figure 3. The research leading to these results has received funding from the European Research Council under the European Union’s Seventh Framework Programme (FP/2007-2013) / ERC Grant Agreement n. 320964 (WDTracer).

REFERENCES

- Adams, F. C., & Bloch, A. M. 2013, *ApJL*, 777, L30
- Adams, F. C., Anderson, K. R., & Bloch, A. M. 2013, *MNRAS*, 432, 438
- Agol, E. 2011, *ApJL*, 731, L31
- Anglada-Escudé, G., Tuomi, M., Gerlach, E., et al. 2013, *A&A*, 556, A126
- Ballard, S., Johnson, J.A. 2014, Submitted to *ApJ*, arXiv:1410.4192
- Barnes, J. W. 2007, *PASP*, 119, 986
- Barnes, R., & Greenberg, R. 2006, *ApJL*, 647, L163
- Barnes, R., & Raymond, S. N. 2004, *ApJ*, 617, 569
- Barnes, R., Goździewski, K., & Raymond, S. N. 2008, *ApJL*, 680, L57
- Barnes, R., & Heller, R. 2013, *Astrobiology*, 13, 279
- Bear, E., & Soker, N. 2013, *New Astronomy*, 19, 56
- Becklin, E. E., Farihi, J., Jura, M., et al. 2005, *ApJL*, 632, L119
- Bergfors, C., Farihi, J., Dufour, P., & Rocchetto, M. 2014, *MNRAS*, 444, 2147
- Bochkarev, K. V., & Rafikov, R. R. 2011, *ApJ*, 741, 36

- Bodman, E. H. L., & Quillen, A. C. 2014, *MNRAS*, 440, 1753
- Bonsor, A., Mustill, A. J., & Wyatt, M. C. 2011, *MNRAS*, 414, 930
- Cabrera, J., Csizmadia, S., Lehmann, H., et al. 2014, *ApJ*, 781, 18
- Casewell, S. L., Dobbie, P. D., Napiwotzki, R., et al. 2009, *MNRAS*, 395, 1795
- Cassan, A., Kubas, D., Beaulieu, J.-P., et al. 2012, *Nature*, 481, 167
- Catalán, S., Isern, J., García-Berro, E., & Ribas, I. 2008, *MNRAS*, 387, 1693
- Chambers, J. E., Wetherill, G. W., & Boss, A. P. 1996, *Icarus*, 119, 261
- Chambers, J. E. 1999, *MNRAS*, 304, 793
- Chatterjee, S., Ford, E. B., Matsumura, S., & Rasio, F. A. 2008, *ApJ*, 686, 580
- Chatterjee, S., & Tan, J. C. 2014, *ApJ*, 780, 53
- Chirikov, B. V. 1979, *Physics Reports*, 52, 263
- Davies, M. B., Adams, F. C., Armitage, P., et al. 2013, *arXiv:1311.6816*
- Debes, J. H., & Sigurdsson, S. 2002, *ApJ*, 572, 556
- Debes, J. H., Hoard, D. W., Wachter, S., Leisawitz, D. T., & Cohen, M. 2011, *ApJS*, 197, 38
- Debes, J. H., Walsh, K. J., & Stark, C. 2012, *ApJ*, 747, 148
- Deck, K. M., Payne, M., & Holman, M. J. 2013, *ApJ*, 774, 129
- Donnison, J. R. 2011, *MNRAS*, 415, 470
- Duncan, M. J., & Lissauer, J. J. 1998, *Icarus*, 134, 303
- de Elía, G. C., Guilera, O. M., & Brunini, A. 2013, *A&A*, 557, A42
- Efroimsky, M., & Makarov, V. V. 2013, *ApJ*, 764, 26
- Faber, P., & Quillen, A. C. 2007, *MNRAS*, 382, 1823
- Faedi, F., West, R. G., Burleigh, M. R., Goad, M. R., & Hebb, L. 2011, *MNRAS*, 410, 899
- Falcon, R. E., Winget, D. E., Montgomery, M. H., & Williams, K. A. 2010, *ApJ*, 712, 585
- Fang, J., & Margot, J.-L. 2013, *ApJ*, 767, 115
- Farihi, J., Jura, M., & Zuckerman, B. 2009, *ApJ*, 694, 805
- Farihi, J., Dufour, P., Napiwotzki, R., & Koester, D. 2011, *MNRAS*, 413, 2559
- Farihi, J., Gänsicke, B. T., Steele, P. R., et al. 2012, *MNRAS*, 421, 1635
- Ford, E. B., & Rasio, F. A. 2008, *ApJ*, 686, 621
- Fossati, L., Bagnulo, S., Haswell, C. A., et al. 2012, *ApJL*, 757, L15
- Frewen, S. F. N., & Hansen, B. M. S. 2014, *MNRAS*, 439, 2442
- Fulton, B. J., Tonry, J. L., Flewelling, H., et al. 2014, *arXiv:1410.0052*
- Funk, B., Wuchterl, G., Schwarz, R., Pilat-Lohinger, E., & Eggl, S. 2010, *A&A*, 516, AA82
- Gänsicke, B. T., Marsh, T. R., Southworth, J., & Rebassa-Mansergas, A. 2006, *Science*, 314, 1908
- Gänsicke, B. T., Marsh, T. R., & Southworth, J. 2007, *MNRAS*, 380, L35
- Gänsicke, B. T., Koester, D., Marsh, T. R., Rebassa-Mansergas, A., & Southworth, J. 2008, *MNRAS*, 391, L103
- Gänsicke, B. T. 2011, *American Institute of Physics Conference Series*, 1331, 211
- Georgakarakos, N. 2008, *Celestial Mechanics and Dynamical Astronomy*, 100, 151
- Giuppone, C. A., Morais, M. H. M., & Correia, A. C. M. 2013, *MNRAS*, 436, 3547
- Goldreich, P. 1966, *AJ*, 71, 1
- Graham, J. R., Matthews, K., Neugebauer, G., & Soifer, B. T. 1990, *ApJ*, 357, 216
- Grimm, S. L., & Stadel, J. G. 2014, *arXiv:1404.2324*
- Hands, T. O., Alexander, R. D., & Dehnen, W. 2014, *MNRAS*, 445, 749
- Hansen, B. M. S., & Murray, N. 2012, *ApJ*, 751, 158
- Hansen, B. M. S., & Murray, N. 2013, *ApJ*, 775, 53
- Hansen, B. M. S., & Murray, N. 2014, *arXiv:1405.2342*, Submitted to *MNRAS*
- Henning, W. G., & Hurford, T. 2014, *ApJ*, 789, 30
- Hogan, E., Burleigh, M. R., & Clarke, F. J. 2009, *MNRAS*, 396, 2074
- Hurley, J. R., Pols, O. R., & Tout, C. A. 2000, *MNRAS*, 315, 543
- Hut, P. 1981, *A&A*, 99, 126
- Johansen, A., Davies, M. B., Church, R. P., & Holmelin, V. 2012, *ApJ*, 758, 39
- Jura, M. 2003, *ApJL*, 584, L91
- Jurić, M., & Tremaine, S. 2008, *ApJ*, 686, 603
- Kaib, N. A., Raymond, S. N., & Duncan, M. 2013, *Nature*, 493, 381
- Kalirai, J. S., Hansen, B. M. S., Kelson, D. D., et al. 2008, *ApJ*, 676, 594
- Kane, S. R., Hinkel, N. R., & Raymond, S. N. 2013, *AJ*, 146, 122
- Kennedy, G. M., & Kenyon, S. J. 2008, *ApJ*, 673, 502
- Kilic, M., von Hippel, T., Leggett, S. K., & Winget, D. E. 2005, *ApJL*, 632, L115
- Koester, D., Girven, J., Gänsicke, B. T., & Dufour, P. 2011, *A&A*, 530, A114
- Koester, D., Gänsicke, B. T., & Farihi, J. 2014, *A&A*, 566, AA34
- Kokubo, E., & Ida, S. 1998, *Icarus*, 131, 171
- Kratter, K. M., & Shannon, A. 2014, *MNRAS*, 437, 3727
- Laskar, J., & Gastineau, M. 2009, *Nature*, 459, 817
- Levison, H. F., Morbidelli, A., Tsiganis, K., Nesvorný, D., & Gomes, R. 2011, *AJ*, 142, 152
- Liebert, J., Bergeron, P., & Holberg, J. B. 2005, *ApJS*, 156, 47
- Lin, H. W., & Loeb, A. 2014, *ApJL*, 793, LL43
- Lissauer, J. J., Fabrycky, D. C., Ford, E. B., et al. 2011, *Nature*, 470, 53
- Lissauer, J. J., Jontof-Hutter, D., Rowe, J. F., et al. 2013, *ApJ*, 770, 131
- Loeb, A., & Maoz, D. 2013, *MNRAS*, 432, L11
- Lovis, C., Ségransan, D., Mayor, M., et al. 2011, *A&A*, 528, A112
- Luhman, K. L., Burgasser, A. J., & Bochanski, J. J. 2011, *ApJL*, 730, LL9
- Mardling, R. A. 2008, *The Cambridge N-Body Lectures*, 760, 59
- Marois, C., Macintosh, B., Barman, T., et al. 2008, *Science*, 322, 1348
- Marois, C., Zuckerman, B., Konopacky, Q. M., Macintosh, B., & Barman, T. 2010, *Nature*, 468, 1080
- Marzari, F. 2014, *MNRAS*, 442, 1110
- Masuda, K. 2014, *ApJ*, 783, 53
- Matsumura, S., Ida, S., & Nagasawa, M. 2013, *ApJ*, 767, 129
- Melis, C., Dufour, P., Farihi, J., et al. 2012, *ApJL*, 751, L4

- Metzger, B. D., Rafikov, R. R., & Bochkarev, K. V. 2012, *MNRAS*, 423, 505
- Mignard, F. 1979, *Moon and Planets*, 20, 301
- Monteiro, H. 2010, *Bol. Soc. Astron. Brasileira*, 29, 22
- Mullally, F., Winget, D. E., De Gennaro, S., et al. 2008, *ApJ*, 676, 573
- Murray, C. D., & Dermott, S. F. 1999, *Solar system dynamics* by Murray, C. D., 1999,
- Mustill, A. J., & Wyatt, M. C. 2012, *MNRAS*, 419, 3074
- Mustill, A. J., & Villaver, E. 2012, *ApJ*, 761, 121
- Mustill, A. J., Veras, D., & Villaver, E. 2014, *MNRAS*, 437, 1404
- Naoz, S., Farr, W. M., Lithwick, Y., Rasio, F. A., & Teyssandier, J. 2013, *MNRAS*, 431, 2155
- Nordhaus, J., & Spiegel, D. S. 2013, *MNRAS*, 432, 500
- Ogilvie, G. I. 2014, *ARA&A*, 52, 171
- Payne, M. J., Deck, K. M., Holman, M. J., & Perets, H. B. 2013, *ApJL*, 775, L44
- Pelupessy, F. I., van Elteren, A., de Vries, N., et al. 2013, *A&A*, 557, A84
- Petrovich, C., Tremaine, S., & Rafikov, R. R. 2014, *ApJ*, 786, 101
- Quillen, A. C. 2011, *MNRAS*, 418, 1043
- Rafikov, R. R. 2011a, *ApJL*, 732, L3
- Rafikov, R. R. 2011b, *MNRAS*, 416, L55
- Rafikov, R. R., & Garmilla, J. A. 2012, *ApJ*, 760, 123
- Raymond, S. N., Barnes, R., Veras, D., et al. 2009a, *ApJL*, 696, L98
- Raymond, S. N., Armitage, P. J., & Gorelick, N. 2009b, *ApJL*, 699, L88
- Raymond, S. N., Armitage, P. J., & Gorelick, N. 2010, *ApJ*, 711, 772
- Raymond, S. N., Armitage, P. J., Moro-Martín, A., et al. 2011, *A&A*, 530, A62
- Raymond, S. N., Armitage, P. J., Moro-Martín, A., et al. 2012, *A&A*, 541, A11
- Reach, W. T., Kuchner, M. J., von Hippel, T., et al. 2005, *ApJL*, 635, L161
- Rein, H., & Spiegel, D. S. 2014, *arXiv:1409.4779*
- Safronov, V. S., & Zvjagina, E. V. 1969, *Icarus*, 10, 109
- Schröder, K.-P., & Connors Smith, R. 2008, *MNRAS*, 386, 155
- Smith, A. W., & Lissauer, J. J. 2009, *Icarus*, 201, 381
- Socrates, A., Katz, B., Dong, S., & Tremaine, S. 2012, *ApJ*, 750, 106
- Steele, P. R., Burleigh, M. R., Dobbie, P. D., et al. 2011, *MNRAS*, 416, 2768
- Swift, J. J., Johnson, J. A., Morton, T. D., et al. 2013, *ApJ*, 764, 105
- Tremblay, P.-E., Ludwig, H.-G., Steffen, M., & Freytag, B. 2013, *A&A*, 559, AA104
- Tsiganis, K., Gomes, R., Morbidelli, A., & Levison, H. F. 2005, *Nature*, 435, 459
- Vassiliadis, E., & Wood, P. R. 1993, *ApJ*, 413, 641
- Veras, D., & Armitage, P. J. 2005, *ApJL*, 620, L111
- Veras, D., & Armitage, P. J. 2006, *ApJ*, 645, 1509
- Veras, D. 2007, *Celestial Mechanics and Dynamical Astronomy*, 99, 197
- Veras, D., & Ford, E. B. 2009, *ApJL*, 690, L1
- Veras, D., Wyatt, M. C., Mustill, A. J., Bonsor, A., & Eldridge, J. J. 2011, *MNRAS*, 417, 2104
- Veras, D., & Moeckel, N. 2012, *MNRAS*, 425, 680
- Veras, D., & Wyatt, M. C. 2012, *MNRAS*, 421, 2969
- Veras, D., & Evans, N. W. 2013a, *Celestial Mechanics and Dynamical Astronomy*, 115, 123
- Veras, D., & Evans, N. W. 2013b, *MNRAS*, 430, 403
- Veras, D., Mustill, A. J., Bonsor, A., & Wyatt, M. C. 2013a, *MNRAS*, 431, 1686
- Veras, D., Hadjidemetriou, J. D., & Tout, C. A. 2013b, *MNRAS*, 435, 2416
- Veras, D., & Mustill, A. J. 2013, *MNRAS*, 434, L11
- Veras, D. 2014, *MNRAS*, 442, L71
- Veras, D., Leinhardt, Z. M., Bonsor, A., Gänsicke, B. T. 2014a, *MNRAS*, 445, 2244
- Veras, D., Shannon, A., Gänsicke, B. T. 2014b, *MNRAS*, 445, 4175
- Veras, D., Evans, N. W., Wyatt, M. C., & Tout, C. A. 2014c, *MNRAS*, 437, 1127
- Veras, D., Jacobson, S.A., Gänsicke, B. T. 2014d, *MNRAS* 445, 2794
- Villaver, E., Livio, M., Mustill, A. J., & Siess, L. 2014, *ApJ*, 794, 3
- Voyatzis, G., Hadjidemetriou, J. D., Veras, D., & Varvoglis, H. 2013, *MNRAS*, 430, 3383
- Wilson, D. J., Gänsicke, B., Koester, D., et al. 2014, *MNRAS*, 445, 1878
- Winn, J. N., & Fabrycky, D. C. 2015, submitted to *ARA&A*, *arXiv:1410.4199*
- Wisdom, J. 1980, *AJ*, 85, 1122
- Wolszczan, A., & Frail, D. A. 1992, *Nature*, 355, 145
- Wolszczan, A. 1994, *Science*, 264, 538
- Wyatt, M. C., Farihi, J., Pringle, J. E., & Bonsor, A. 2014, *MNRAS*, 439, 3371
- Xu, S., & Jura, M. 2014, *ApJL*, 792, LL39
- Zakamska, N. L., & Tremaine, S. 2004, *AJ*, 128, 869
- Zhou, J.-L., Lin, D. N. C., & Sun, Y.-S. 2007, *ApJ*, 666, 423
- Zuckerman, B., Koester, D., Reid, I. N., Hünsch, M. 2003, *ApJ*, 596, 477
- Zuckerman, B., Melis, C., Klein, B., Koester, D., & Jura, M. 2010, *ApJ*, 722, 725
- Zuckerman, B., & Becklin, E. E. 1987, *Nature*, 330, 138